Available online at www.sciencedirect.com
SCIENCE DIRECT
Tetrahedron 62 (2006) 352–356
Tetrahedron

Kinetic isotope and thermodynamic analysis of the nornicotine-catalyzed aqueous aldol reaction

Claude J. Rogers, Tobin J. Dickerson and Kim D. Janda*

Departments of Chemistry and Immunology and The Skaggs Institute for Chemical Biology, The Scripps Research Institute, 10550 North Torrey Pines Road, La Jolla CA 92037, USA

Received 5 July 2005; revised 17 August 2005; accepted 9 September 2005

Available online 11 October 2005

Abstract—A series of kinetic isotope effects and thermodynamic studies were performed to test key predictions of a computationally derived model for a nornicotine-catalyzed aqueous aldol reaction. The relative energies of the two computationally-derived transition states were challenged using the proton inventory, which demonstrated that a single water molecule from the solvent is involved in, or before, the rate-limiting step. These results suggest the importance of proton transfer in the aqueous aldol reaction and may assist the development of other aqueous organocatalytic processes.
© 2005 Elsevier Ltd. All rights reserved.

1. Introduction

Recently, organocatalysis has become an increasingly useful tool in the construction of complex molecular skeletons.[1] The intense interest in the field has led to the development of a wide variety of catalysts capable of accelerating a diverse set of reactions including aldol additions,[2] Mannich reactions,[3] [4+2][4] and [3+2][5] cycloadditions, α-aminations,[6] epoxidations,[7] and cyclopropanations.[8] Despite this flurry of activity, there are few examples of truly aqueous organocatalysts.[9] The development of synthetically viable aqueous organocatalysts would be a boon to the field of green chemistry, assisting the development of environmentally benign chemical processes. In our laboratory, we have shown that nornicotine **1**, a metabolite of nicotine and constituent of tobacco, can catalyze aqueous aldol reactions under physiologically relevant conditions (Scheme 1).[10] Aside from the pharmacological implications,[11] this reaction is noteworthy because it was the first, and still one of the few, examples of non-enzymatic aqueous enamine-based chemistry.[9] While the reaction proceeds in good yield with sufficiently activated substrates, the rate and substrate compatibility of the reaction must be improved before it can be considered synthetically useful. With these thoughts in mind, we recently initiated a research program aimed at explicating the mechanism of this reaction to better understand the molecular basis for rate enhancement, and thus develop improved aqueous organocatalysts.

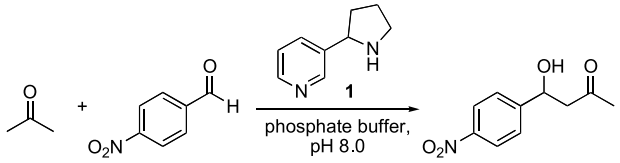

Scheme 1. An aqueous aldol reaction catalyzed by 30 mol % nornicotine **1** in 200 mM phosphate buffer at 37 °C.

To elucidate the structural requirements for effective catalysis, a series of nornicotine analogs were used to determine the linear free energy relationship between small changes in the structure of the catalyst and the rate of the reaction.[12] By replacing nornicotine with *meta* and *para* substituted 2-arylpyrrolidines, the rate of the reaction increased with a corresponding increase in the electron-withdrawing nature of the substituents on the aryl ring of the catalyst. The positive value of the slope of the Hammett plot, ρ, may be due to the lower pK_a of the pyrrolidine nitrogen of analogs containing electron-withdrawing groups on the aryl ring. Thus, the perturbed pK_a of these analogs effectively increases the amount of available catalyst under the reaction conditions. While these results explained why proline (predominantly zwitterionic at pH 8.0) and pyrrolidine (pK_a=11.4) are poor aqueous organocatalysts, it did not give insight into why the nornicotine-catalyzed aldol reaction similarly fails in organic solvent.[9,10]

Keywords: Nornicotine; Organocatalysis; Kinetic isotope effects.
* Corresponding author. Tel.: +1 858 784 2515; fax: +1 858 784 2595; e-mail: kdjanda@scripps.edu

0040–4020/$ - see front matter © 2005 Elsevier Ltd. All rights reserved.
doi:10.1016/j.tet.2005.09.094

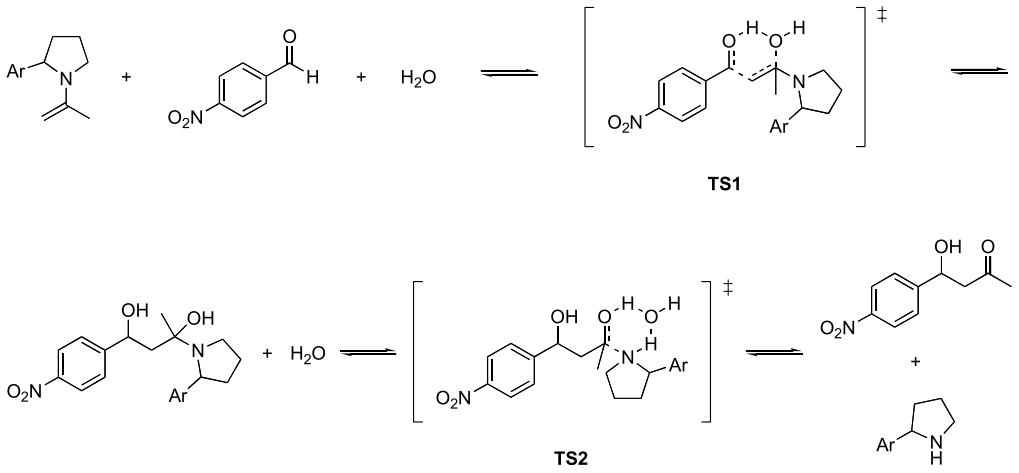

Scheme 2. A computationally derived mechanism for a nornicotine-catalyzed aldol reaction in water.

A rational explanation of this phenomenon is that an explicit proton must transfer at the transition state for the reaction to occur. This explanation was supported by the results of a computational study into the mechanism of the nornicotine-catalyzed aqueous aldol reaction.[13] In this study, the calculations were simplified by assuming that the enamine was preformed, and the energy of the enamine was the zero-point for the reaction. Based on this assumption, the predicted mechanism revealed that, unlike an aldol reaction in organic solvent, the reaction proceeds through a two-step mechanism, with each step requiring an explicit water molecule from the solvent (Scheme 2). Carbon–carbon bond formation proceeds through a trimolecular six-membered transition state **TS1** and forms a stable, albeit short-lived, hemiaminal intermediate. The rate-limiting step is hydrolysis of the hemiaminal via **TS2** to give the product with concomitant regeneration of the catalyst.

Although the trimolecular **TS1** is unusual and would seem to be entropically unfavorable, there is empirical evidence that the concerted transfer of a proton in the transition state is important. For example, the calculations for the uncatalyzed reaction required proton transfer in the transition state for both organic and aqueous media. Considering that a hydrogen-bound water could activate the aldehyde for nucleophilic attack, and the large excess of water in the reaction ($\sim$55 M), the assumption of an explicitly involved water molecule is reasonable. Furthermore, there is evidence for a trimolecular transition state involving water in the aqueous Diels–Alder reaction of methyl vinyl ketone and cyclopentadiene.[14] Analogous to the proposed mechanism for the nornicotine-catalyzed aqueous aldol reaction, water accelerates the reaction by acting as a Lewis acid by providing a hydrogen bond to methyl vinyl ketone. We report herein upon a series of kinetic isotope and thermodynamic experiments designed to help determine the validity of the computationally derived mechanism for the nornicotine-catalyzed aqueous aldol reaction.

2. Results and discussion

A key prediction of the computational mechanism is that two explicit water molecules from the solvent are involved in, or before, the rate-limiting step. Therefore, the rate of the reaction in deuterium oxide should be significantly reduced relative to the rate of the reaction in water, as two O–(D) bonds should be broken based on this prediction. The isotope effect was determined in buffered water and buffered deuterium oxide.[15] Rate constants were measured under pseudo-first-order conditions by using acetone as the donor and 4-nitrobenzaldehyde as the acceptor. Experiments were performed at 37 °C, under conditions in which the reaction rate was maximized relative to the uncatalyzed reaction (pH 8.0). While a large isotope effect was predicted based upon the proposed computational mechanism, the measured value ($k_H/k_D \approx 3$) was surprisingly small. To provide an explanation for the magnitude of the kinetic isotope effect, the number of water molecules involved in the reaction, the proton inventory, was determined by observing the effect of increasing the atom fraction of deuterium (n) on the corresponding observed rate constant (k_n). In addition to the number of protons from the solvent involved in the transition state, the transition state fractionation factors can be calculated for the reaction.[16] The fractionation factor (ϕ) is a measure of the preference of the solute (SH) for combination with deuterium, relative to water (ROH),[17] that is,

$$\phi = \frac{[\mathrm{SD}]/[\mathrm{SH}]}{[\mathrm{ROD}]/[\mathrm{ROH}]}$$

The proton inventory requires application of the Gross–Butler Eq. (1),

$$k_n = k_H \frac{\prod_{i}^{\text{Transition state}} (1 - n + n\phi_i)}{\prod_{j}^{\text{Reaction state}} (1 - n + n\phi_j)} \quad (1)$$

where ϕ_i and ϕ_j are the fractionation factors for all exchangeable hydrogens in the transition state and reactant state, respectively. According to the proposed mechanism, the two protons from water in **TS1** and **TS2** show a change between reagent and transition state, thus Eq. (1) simplifies to give,

$$k_n = k_H(1 - n + n\phi^{\ddagger}_{TS1})(1 - n + n\phi^{\ddagger}_{TS2}) \quad (2)$$

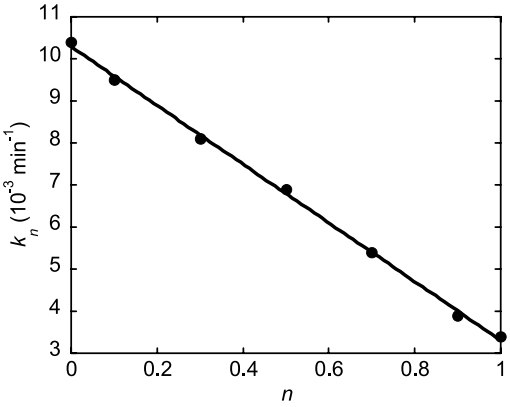

Figure 1. Proton inventory for the nornicotine-catalyzed aqueous aldol reaction. The magnitude of the error bars are obscured by the corresponding point.

where $\phi^{\ddagger}$ is the transition-state fractionation factor. Therefore, the theoretical mechanism predicts a non-linear dependence between k_n and n.

In contrast to the predicted dependence, a plot of the observed rate constant versus increasing atom fraction of deuterium was linear ($R^2=0.999$, Fig. 1), indicating only one water molecule from the solvent is involved in the transition state. Therefore, a key prediction of the computational mechanism appears to be incorrect. When applied to the data, the Gross–Butler equation simplifies to give,

$$k_n = k_H(1-n+n\phi^{\ddagger}) \tag{3}$$

consistent with the involvement of a single water molecule, with $\phi^{\ddagger}=0.32$. In this case, the value of the transition state fractionation factor is also the inverse of the isotope effect.

Having established that a single water molecule participates in the reaction at or prior to the rate-limiting step, we considered the implications of the magnitude of the primary kinetic isotope effect, as the value is significantly lower than the theoretical maximum. An explanation for this reduction is that isotope effects are lower for proton transfer between two oxygen atoms than for a transfer from oxygen to carbon.[16] However, the magnitude of the isotope effect also depends on the geometry of the transition state. Isotope effects are maximized when the geometry of the proton-in-flight during the transition state approaches linearity. Interestingly, the reduced isotope effect is consistent with the predicted geometry of both six-membered transition states **TS1** and **TS2**, as the bond angles required ($\sim$109°) would lower the magnitude of the isotope effect.[18]

While the results of proton inventory experiment are contradictory with the predicted involvement of two molecules of water involved in or before the rate-limiting step, these results provide evidence that one molecule of water is involved in the reaction, and are consistent with the proposed six-membered transition state. Furthermore, these results are in accord with the computational mechanism, provided the relative energies are inaccurate as a result of the lack of entropic corrections in the computational

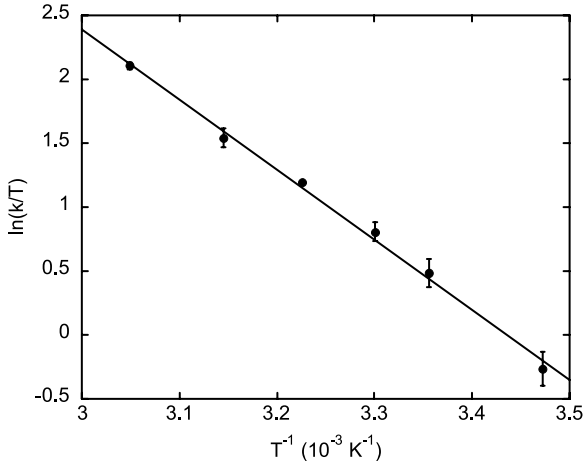

Figure 2. Eyring analysis for the nornicotine-catalyzed aqueous aldol reaction evaluated over a range of temperatures between 15–55 °C.

experiments. Provided that $\Delta G_{TS1} > \Delta G_{TS2}$ upon inclusion of the entropic penalties in the calculation, the results of the proton inventory are entirely consistent with the proposed mechanism. Since **TS1** requires ordering three molecules, the entropic penalty is expected to be larger than the penalty for **TS2**, thus it is possible that their inclusion could make the first step rate limiting.

To further characterize the mechanism, the activation parameters $\Delta S^{\ddagger}$ and $\Delta H^{\ddagger}$ were calculated. Measuring the rate of the reaction at different temperatures allowed for the application of the Erying equation,

$$\ln(k) = \frac{\Delta S^{\ddagger}}{R} + \ln\left(\frac{k_B}{h}\right) - \frac{\Delta H^{\ddagger}}{RT} \tag{4}$$

where k_B and h are the Boltzman and Planck's constants, respectively. The plot of $\ln(k/T)$ versus $1/T$ was found to be linear over the range of temperatures examined ($R^2=0.996$, Fig. 2). The calculated value of $\Delta S^{\ddagger}$ was -9.8 ± 1.2 cal K^{-1} mol^{-1} and $\Delta H^{\ddagger}$ was 10.9 ± 0.4 kcal mol^{-1}. While the value of $\Delta S^{\ddagger}$ is negative, as predicted, it is not possible to make any mechanistic determinations based on the sign or the magnitude of the value without a reference reaction of the same standard state.[19]

Further investigation into the mechanistic assumptions was provided by isotopic substitution of the hydrogens at reactive centers of the aldehyde and acetone. For example, an inverse α-secondary kinetic isotope effect was expected upon isotopic substitution of the aldehydic proton due to the $sp^2 \rightarrow sp^3$ transition at the reactive carbon. The effect of this substitution was measured with 4-nitro-(α-d_1)benzaldehyde, synthesized according to a known procedure.[20] Indeed, the deuterated aldehyde perturbed the rate of the reaction by a magnitude consistent with an inverse secondary isotope effect (Table 1).

Upon substitution of acetone with d_6-acetone, a primary isotope effect was observed due to C–(D) bond cleavage when forming the enamine. Additionally, the hybridization change at the enamine methylene after carbon–carbon bond formation should result in an inverse secondary kinetic isotope effect. However, the magnitude of the effect was

Table 1. Summary of kinetic and thermodynamic parameters for the nornicotine-catalyzed aqueous aldol reaction

Entry	Parameter	Value[a]
1	k_H/k_D (Water)	3.05 ± 0.10
2	k_H/k_D (aldehyde)	0.89 ± 0.08
3	k_H/k_D (acetone)	4.76 ± 0.11
4	$\phi^{\ddagger}$	0.32 ± 0.01
5	$\Delta S^{\ddagger}$	-9.8 ± 1.2[b]
6	$\Delta H^{\ddagger}$	10.9 ± 0.4[c]

[a] Error for all parameters determined by propagation of error analysis.
[b] Value given in cal K^{-1} mol^{-1}.
[c] Value given in kcal mol^{-1}.

obscured by the primary isotope effect. Considering multiple isotope effects are assumed to be additive, we attempted to deconvolute the secondary kinetic isotope effect by directly measuring the observed K_{eq} of enamine formation via 2D ^1H–^1H ROESY and NOESY NMR spectroscopy. Unfortunately, the error associated with the measurement was too large to calculate a reasonable equilibrium constant as the diagonal peak of the enamine methyl overlapped substantially with adjacent nornicotine peaks of much greater intensity (data not shown). Nonetheless, the results of the acetone and aldehyde kinetic isotope effects indicate that carbon–carbon bond and enamine formation occur in or before the rate-limiting step, consistent with the proposed mechanism.

3. Conclusion

Based on the data obtained in this study, we are able to reject the relative energies of the computationally derived mechanism for the nornicotine-catalyzed aqueous aldol reaction. Provided **TS1** is the rate-limiting step, the data is entirely in accord with the computational mechanism. However, this does not preclude other mechanistic possibilities that are also consistent with the data. While we were not able to provide evidence to directly support the proposed trimolecular transition state, these results underscore the importance of proton transfer in aldol organocatalysis, as the nornicotine-catalyzed reaction fails in organic solvent most likely because there are few available protons to participate in the transition state. Combined with our previous results,[12] we are able to provide a clearer picture into the mechanistic demands of the aqueous aldol reaction, which should assist in the development of future green organocatalysts.

4. Experimental

4.1. General methods

All chemicals were obtained from commercial suppliers. Nornicotine was distilled prior to use. HPLC solvents were filtered and degassed prior to use. All isotopic solvents and reagents were above 99.9% enrichment, if available, otherwise the highest commercially available enrichment was used. All HPLC experiments were preformed using a C_{18} reverse-phase column and an isocratic mobile phase of 25% acetonitrile in water with 0.1% TFA, with a flow rate of 1.0 mL min^{-1}, monitoring at 254 nm. Product formation was followed by monitoring the height and area of the peak corresponding to 4-hydroxy-4-(4-nitrophenyl)butan-2-one ($t_R = 6.2$ min) and extrapolating concentrations from a standard curve obtained using a synthetic standard.[21]

4.2. General procedure for kinetic experiments

Nornicotine was added as a 300 mM solution in DMSO to a solution of 200 mM phosphate buffer (pH 8.0) and acetone. The solution was briefly vortexed, and then incubated at 37 °C. The reaction was initiated by the addition of 4-nitrobenzaldehyde as a 100 mM solution in DMSO. The final concentrations of reactants were 2.4 mM nornicotine, 240 mM acetone, and 1–8 mM 4-nitrobenzaldehyde in 10% DMSO. The progress of the reaction was monitored by removing 10 μL aliquots of the solution at various times during the reaction and diluting them to a total volume of 500 μL. Then, 20 μL of these samples were injected onto an analytical RP-C18 HPLC column for analysis. Pseudo-first-order rate constants were determined by linear regression analysis.

4.3. General procedure for kinetic isotope experiments

Kinetic isotope effects were measured by substituting the appropriate amount of deuterated substrate into the reaction. The observed rate constant (k_D) was then compared to the rate of the reaction with only protiated substrates (k_H). The proton inventory was determined by measuring the observed rate constant at increasing percent of phosphate buffered D_2O (200 mM potassium phosphate, pD 8.0)[16] in phosphate buffered H_2O (200 mM potassium phosphate, pH 8.0).

Acknowledgements

We thank the reviewer for valuable suggestions and gratefully acknowledge financial support from The Skaggs Institute for Chemical Biology.

References and notes

1. Dalko, P. I.; Moisan, L. *Angew. Chem., Int. Ed.* **2004**, *43*, 5138–5175.
2. For examples, see: (a) Pidathala, C.; Hoang, L.; Vignola, N.; List, B. *Angew. Chem., Int. Ed.* **2003**, *42*, 2785–2788. (b) Peng, Y.-Y.; Ding, Q.-P.; Li, Z.; Wang, P.-G.; Cheng, J.-P. *Tetrahedron Lett.* **2003**, *44*, 3871–3875. (c) Córdova, A.; Notz, W.; Barbas, C. F., III *J. Org. Chem.* **2002**, *67*, 301–303.
3. Córdova, A. *Acc. Chem. Res.* **2004**, *37*, 102–112.
4. (a) Juhl, K.; Jørgensen, K. A. *Angew. Chem., Int. Ed.* **2003**, *42*, 1498–1501. (b) Thayumanavan, R.; Dhevalapally, B.; Sakthivel, K.; Tanaka, F.; Barbas, C. F., III *Tetrahedron Lett.* **2002**, *43*, 3817–3820. (c) Ramchary, D. B.; Chowdari, N. S.; Barbas, C. F., III *Angew. Chem., Int. Ed.* **2003**, *42*, 4233–4237.
5. (a) Jen, W. S.; Wiener, J. J. M.; MacMillan, D. W. C. *J. Am. Chem. Soc.* **2000**, *122*, 9874–9875. (b) Karlsson, S.; Högberg, H. E. *Tertahedron: Asymmetry* **2002**, *13*, 941–945.
6. Duthaler, R. O. *Angew. Chem., Int. Ed.* **2003**, *42*, 975–978.

7. (a) Marigo, M.; Franzén, J.; Plousen, T. B.; Zhuang, W.; Jørgensen, K. A. *J. Am. Chem. Soc.* **2005**, *127*, 6964–6965. (b) Aggarwal, V. K.; Lopin, C.; Sandrinelli, F. *J. Am. Chem. Soc.* **2003**, *125*, 7596–7601.
8. Kunz, R. K.; MacMillan, D. W. C. *J. Am. Chem. Soc.* **2005**, *127*, 3240–3241.
9. For other examples, see: (a) Reymond, J.-L.; Chen, Y. *J. Org. Chem.* **1995**, *60*, 6970–6979. (b) Cordova, A.; Notz, W.; Barbas, C. F., III *Chem. Commun.* **2002**, 3024–3025. (c) Hatikka, A.; Arvidsson, P. I. *Tetrahedron: Asymmetry* **2004**, *15*, 1831–1834. (d) Chimni, S. S.; Mahajan, D. *Tetrahedron* **2005**, *61*, 5019–5025.
10. Dickerson, T. J.; Janda, K. D. *J. Am. Chem. Soc.* **2002**, *124*, 3220–3221.
11. (a) Dickerson, T. J.; Janda, K. D. *Proc. Natl. Acad. Sci. U.S.A.* **2002**, *99*, 15084–15088. (b) Dickerson, T. J.; Janda, K. D. *Proc. Natl. Acad. Sci. U.S.A.* **2003**, *100*, 8182–8187.
12. Rogers, C. J.; Dickerson, T. J.; Brogan, A. P.; Janda, K. D. *J. Org. Chem.* **2005**, *70*, 3705–3708.
13. Dickerson, T. J.; Lovell, T.; Meijler, M. M.; Noodleman, L.; Janda, K. D. *J. Org. Chem.* **2004**, *69*, 6603–6609.
14. (a) Blake, J. F.; Jorgensen, W. L. *J. Am. Chem. Soc.* **1991**, *113*, 7430–7432. (b) Blake, J. F.; Lim, D.; Jorgensen, W. L. *J. Org. Chem.* **1994**, *59*, 803–805.
15. The relationship, $pD = pH_{obs} + 0.6$, was used to determine the pD of buffered D_2O solutions.
16. Schowen, R. L. *Prog. Phys. Org. Chem.* **1972**, *9*, 275–332.
17. Gold, V. *Adv. Phys. Org. Chem.* **1969**, *7*, 295–331.
18. Chiao, W. B.; Saunders, W. H. *J. Am. Chem. Soc.* **1978**, *100*, 2802–2805.
19. Carpenter, B. K. *Determination of organic reaction mechanisms*; Wiley: New York, 1984.
20. Spletstoser, J. T.; White, J. M.; Georg, G. I. *Tetrahedron Lett.* **2004**, *45*, 2787–2789.
21. List, B.; Lerner, R. A.; Barbas, C. F.; III *J. Am. Chem. Soc.* **2000**, *122*, 2395–2396.